TECHNISCHE UNIVERSITÄT DARMSTADT

INSTITUTE FOR MATERIALS SCIENCE

Defect structure and oxygen diffusion in PZT ceramics

Adam Georg Balogh

Institute of Materials Science

Technische Universität Darmstadt

Introduction

Ferroelectrics are of great technical interest because of their **sensing and actuator properties** e.g.:

- **„smart materials"** (e.g. change of damping behavior)
- thin films for **non-volatile memory applications**

However, the materials suffer from fatigue !
(mechanically and electrically)

electrical fatigue under polarization reversal is attributed to **the hindrance of domain wall mobility with point defects** and electrochemical degradation

The exact fatigue mechanisms are still poorly understood

Consequently, the investigation of point defects and their diffusion are of great interest

Positron Annihilation Spectroscopy

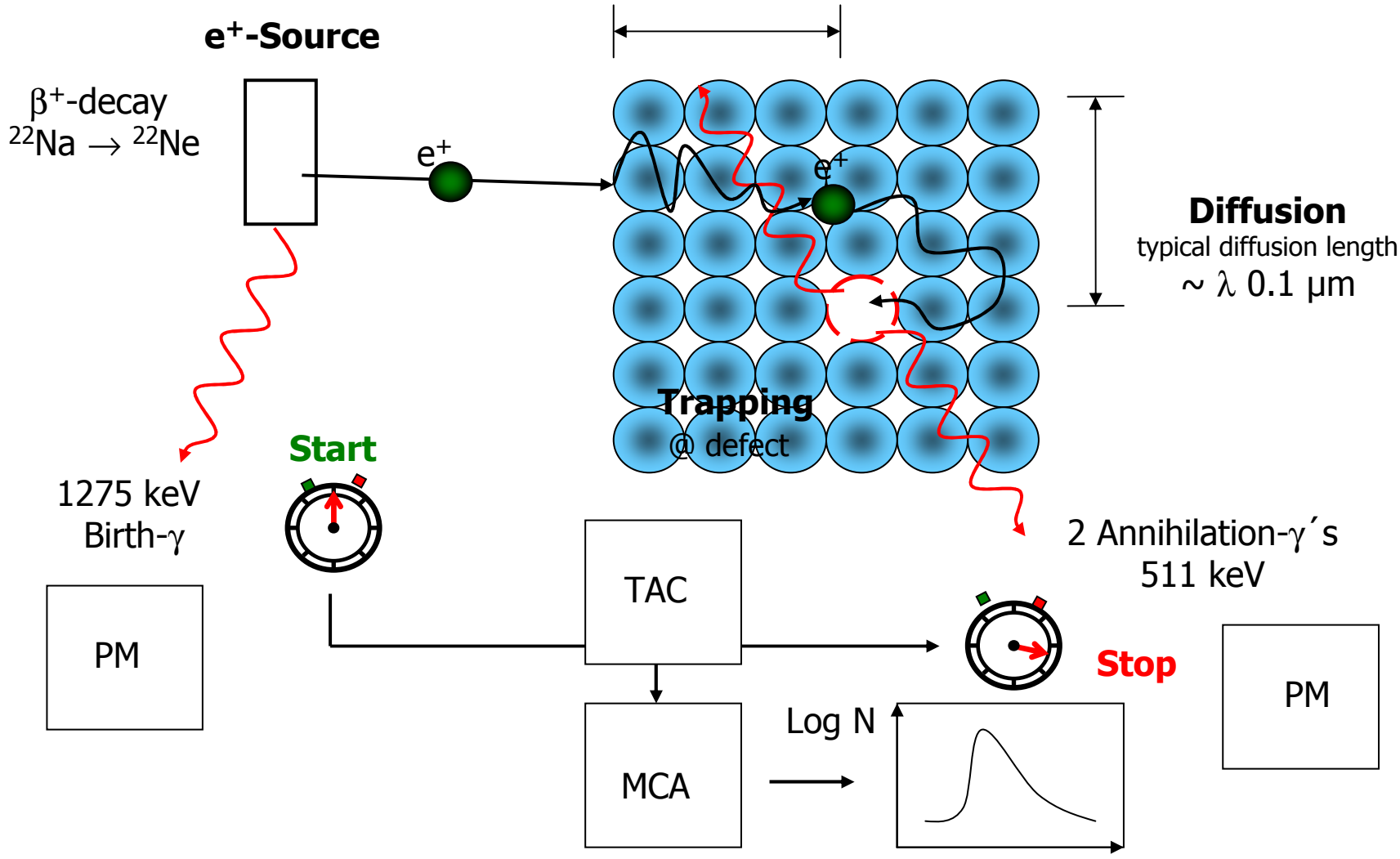

Trapping model

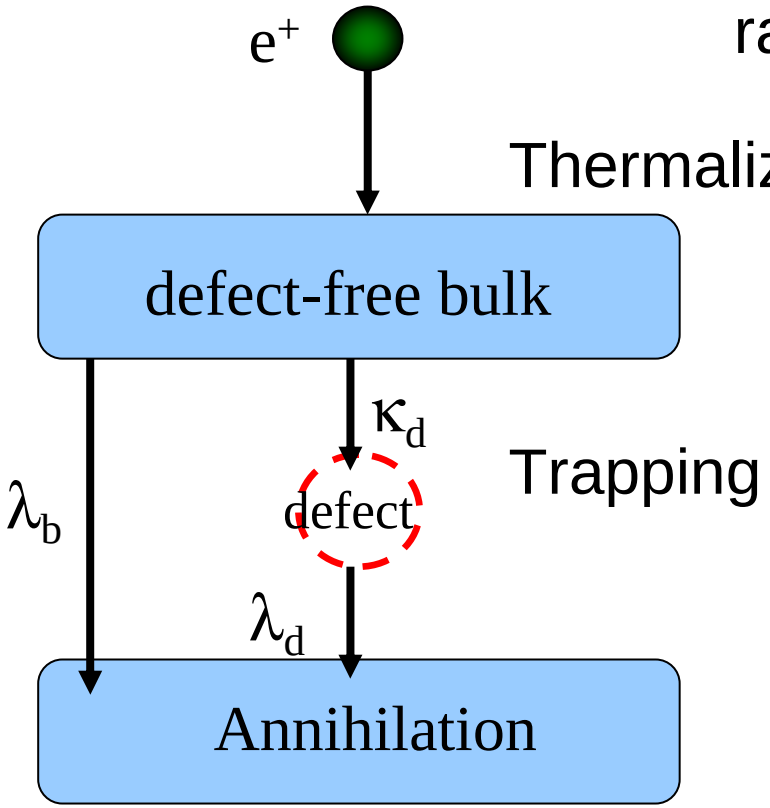

e. g. for a single defect

rate eq.:

$$\frac{d\,n_b}{d\,t} = -\lambda_b n_b - \kappa_d n_b$$

$$\frac{d\,n_d}{d\,t} = -\lambda_d n_d + \kappa_d n_b$$

$$D(t) = I_1 \exp(-\frac{t}{\tau_1}) + I_2 \exp(-\frac{t}{\tau_2})$$

$$\kappa_d = \mu C = I_2\left(\frac{1}{\tau_1} - \frac{1}{\tau_2}\right) = \frac{I_2}{I_1}\left(\frac{1}{\tau_b} - \frac{1}{\tau_d}\right)$$

$$\tau_2 = \frac{1}{\lambda_d}\,; \qquad \tau_1 = \frac{1}{\lambda_b + \kappa_d}$$

Typical Lifetime Spectrum

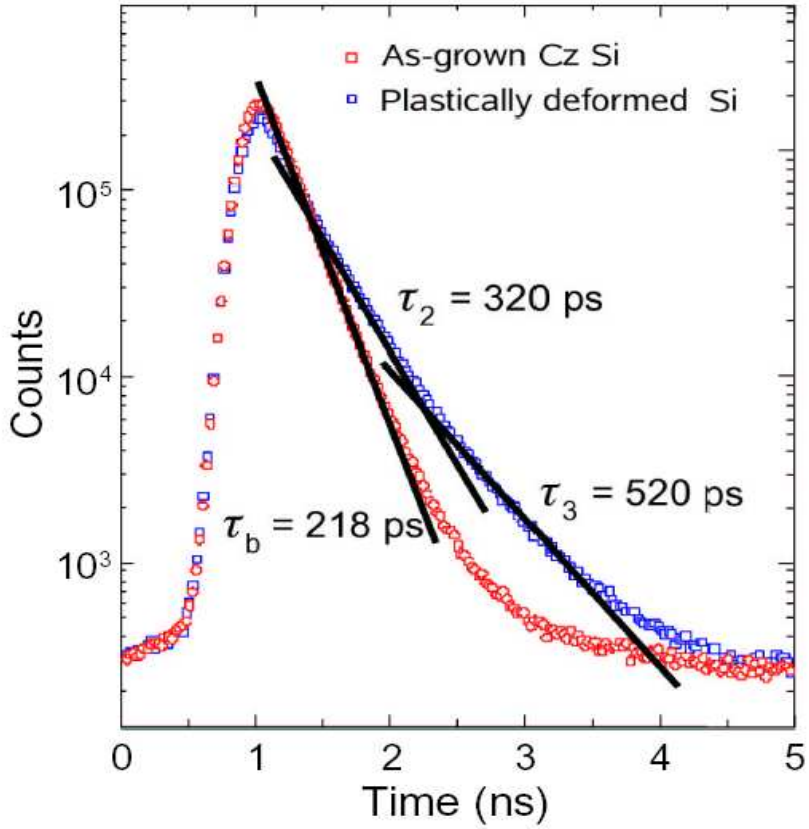

H. S. Leipner, C. G. Hübner, T. E. M. Staab, R. Krause-Rehberg, Mater. Sci. Forum **363-365** (2001), 61-63

The lifetime spectrum is given by:

$$N(t) = \sum_{i=1}^{k+1} \frac{I_i}{\tau_i} \cdot \exp\left\{-\frac{t}{\tau_i}\right\}$$

k defects yield to *k+1* Lifetime-components τ_{k+1} !

Ionic Radii

	Pauling [pm]	4-coordinate [pm]	6-coordinate [pm]	8-coordinate [pm]
Pb^{2+}	120	-	133	143
La^{3+}	115	-	117.2	130
Zr^{4+}	80	73	86	98
Ti^{4+}	68	56	74.5	88
Nb^{5+}	70	62	-	88

[1] www.webelements.com
[2] R.D. Shannon, *Acta Cryst.*, 1976, **A32**, 751.
[3] R.D. Shannon and C.T. Prewitt, *Acta Cryst.*, 1969, **B25**, 925.
[4] R.D. Shannon and C.T. Prewitt, *Acta Cryst.*, 1970, **B26**, 1046.
[5] J.E. Huheey, E.A. Keiter, and R.L. Keiter in , 4th edition, HarperCollins, New York, USA, 1993.

Effect of La^{+3} and Nb^{+5} -doping

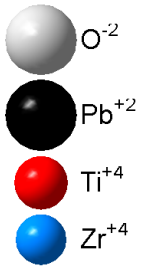

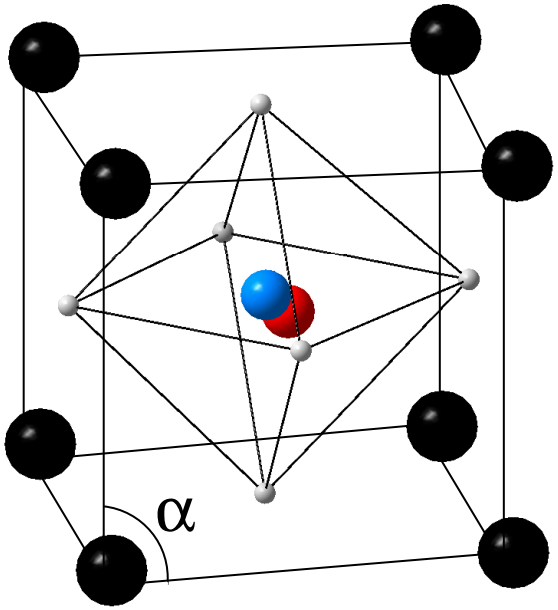

a_0 : 4.102 Å
α,β,γ : 89.68°

Pb^{+2}-site
ionic radii:
$r(La^{+3})/r(Pb^{+2})$~0.88
$r(Nb^{+5})/r(Pb^{+2})$~0.62
the dopant induces V_{Pb}

Zr^{+4}/Ti^{+4}-site
ionic radii:
$r(Nb^{+5})/r([Zr_{60}Ti_{40}]^{+4})$~0.94 the dopant induces V_{Pb}
$r(La^{+3})/ r([Zr_{60}Ti_{40}]^{+4})$~1.38
dopant induces V_O

Cell metric from Rietveld refinement

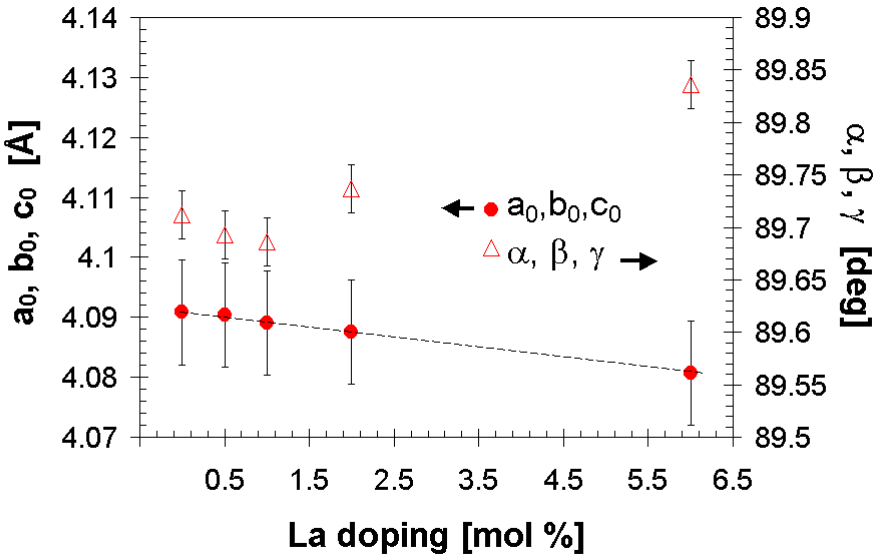

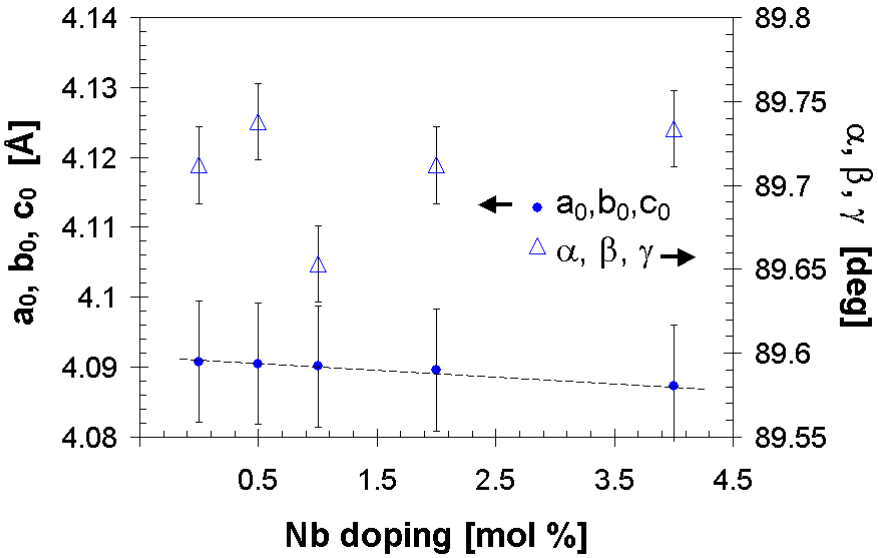

The lattice parameter a_0 as well as the cell volume monotonically decreases for both La^{+3} and Nb^{+5} doping.

According to the ionic radii this suggests that La^{+3} occupies Pb-sites and Nb^{+5} Zr/Ti-sites exclusively.

Cell volume

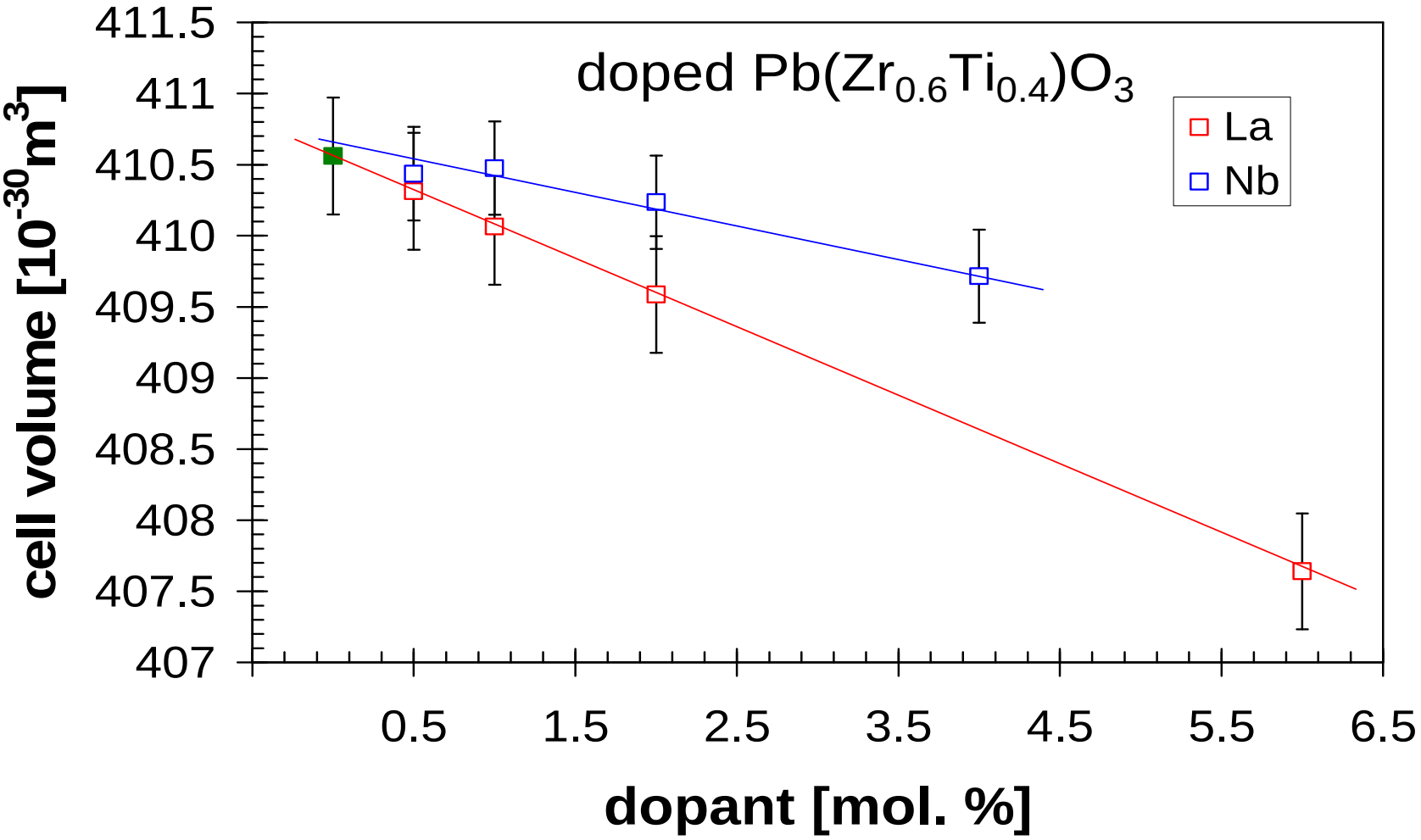
doped Pb(Zr0.6Ti0.4)O3
La
Nb
cell volume [10-30m3]
411.5
411
410.5
410
409.5
409
408.5
408
407.5
407
0.5
1.5
2.5
3.5
4.5
5.5
6.5
dopant [mol. %]

Defect Chemistry

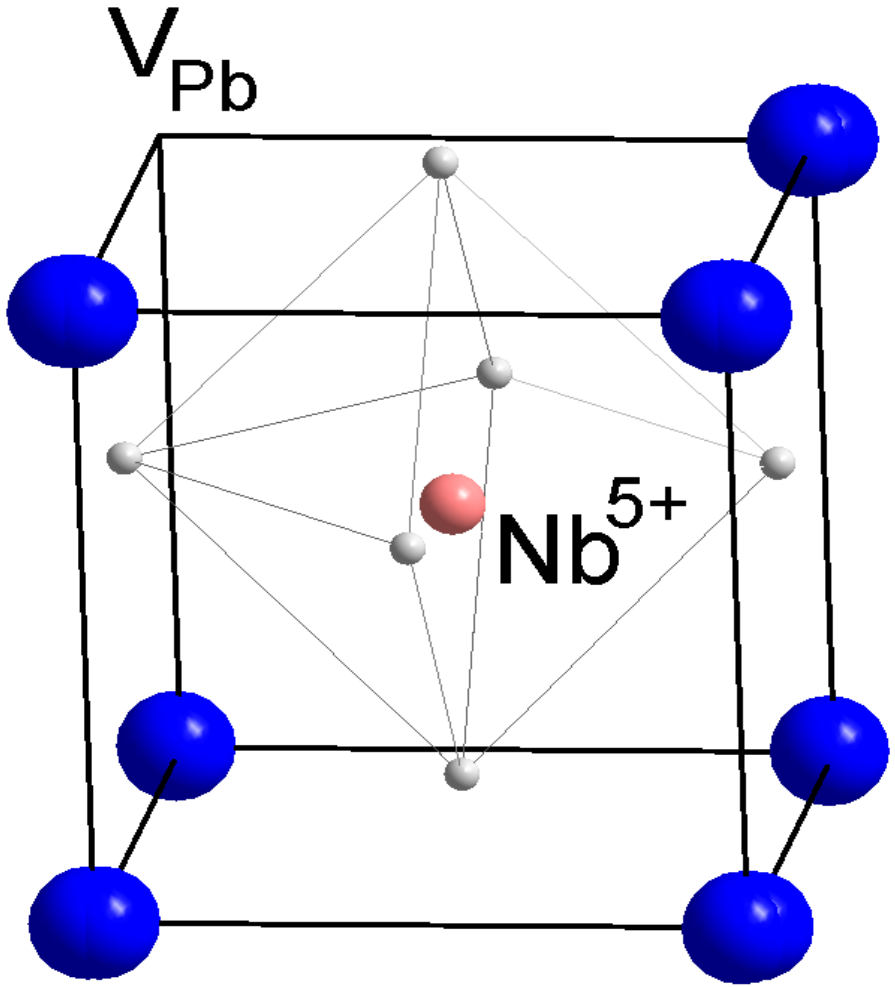

La^{3+} on Pb^{2+} site
$\Rightarrow 2\ La_A \Rightarrow V_{Pb}$

Nb^{5+} on Zr/Ti^{4+} site
$\Rightarrow$ 2 $Nb_B \Rightarrow$ V_{Pb}

Calculated Positron Lifetimes

DFT-pseudopotential, atomic superposition methods

	$PbTiO_3$* τ / [ps]	$LaCoO_3$* τ / [ps]	$BaTiO_3$* τ / [ps]	PZT(60/40) τ / [ps]
bulk	147	129	152	168
V_A	280	275	293	270
V_B	175	173	204	195
V_O	152	145	162	163
$2V_O$		160		
V_AV_O	284	280		305

* V.J. Ghosh, B. Nielsen and Th. Friessnegg, Phys. Rev. B Vol. 61 No. 1 (2000), 207-211

This work with W. Puff and G. Bischoff, TU Graz

Varying Zr/Ti ratio

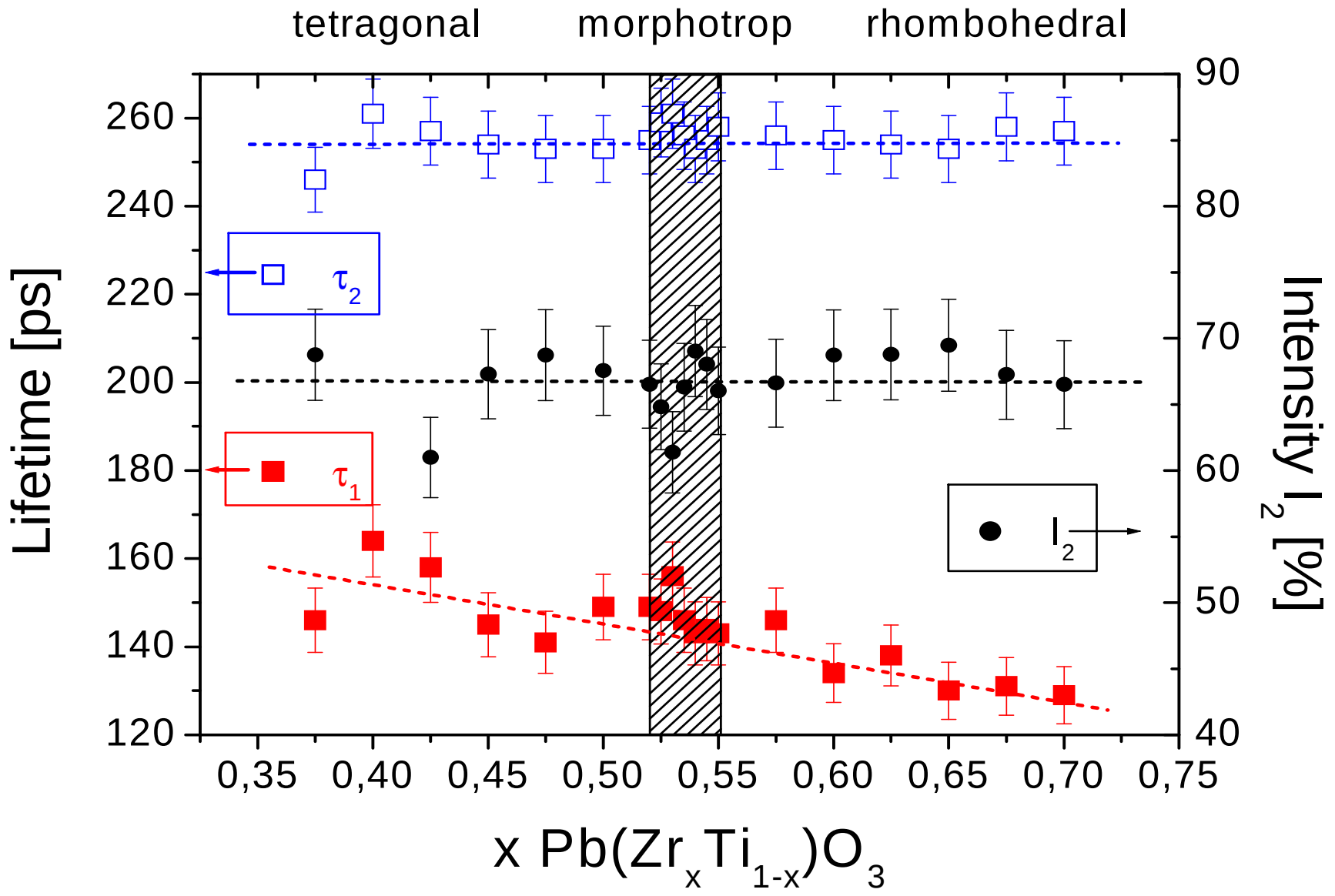

Lifetime data of donor doped samples

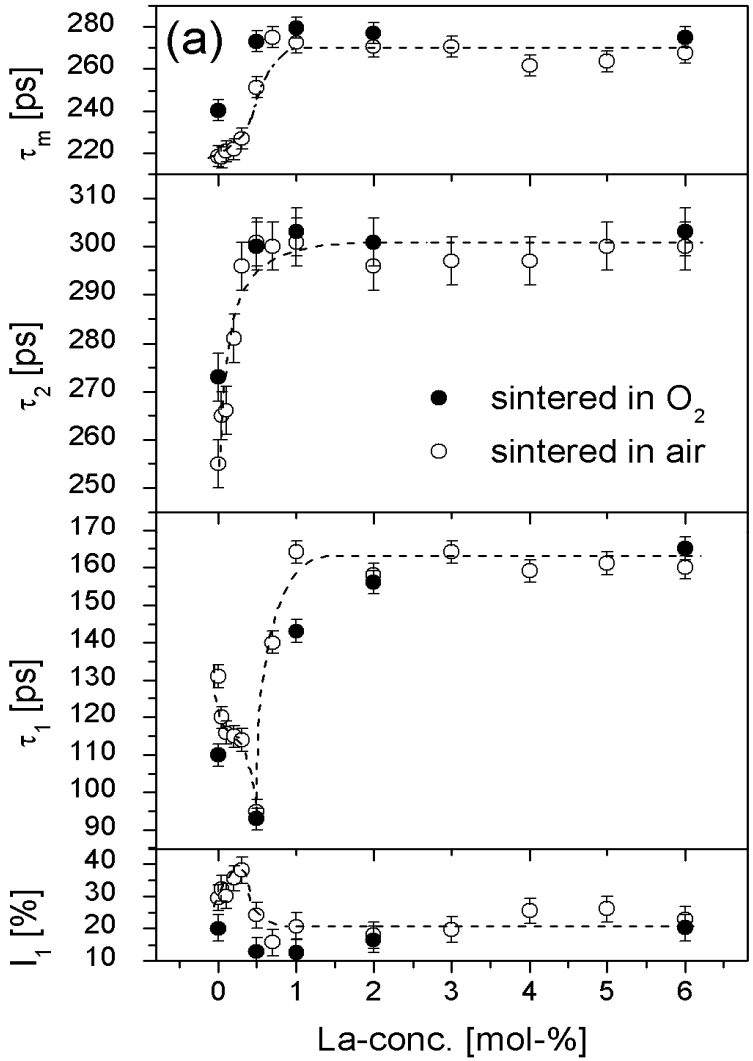

- **donor doping** yields to the saturation of lifetime component τ_2 ~300ps ($\mathbf{V_{Pb}}$)
- τ_2 **255-305 ps**
- as τ_2 saturates, τ_{bulk} disappears, sat. τ_1 can be attributed to $\mathbf{V_O}$ **τ~170 ps**

XPS Pb 4f

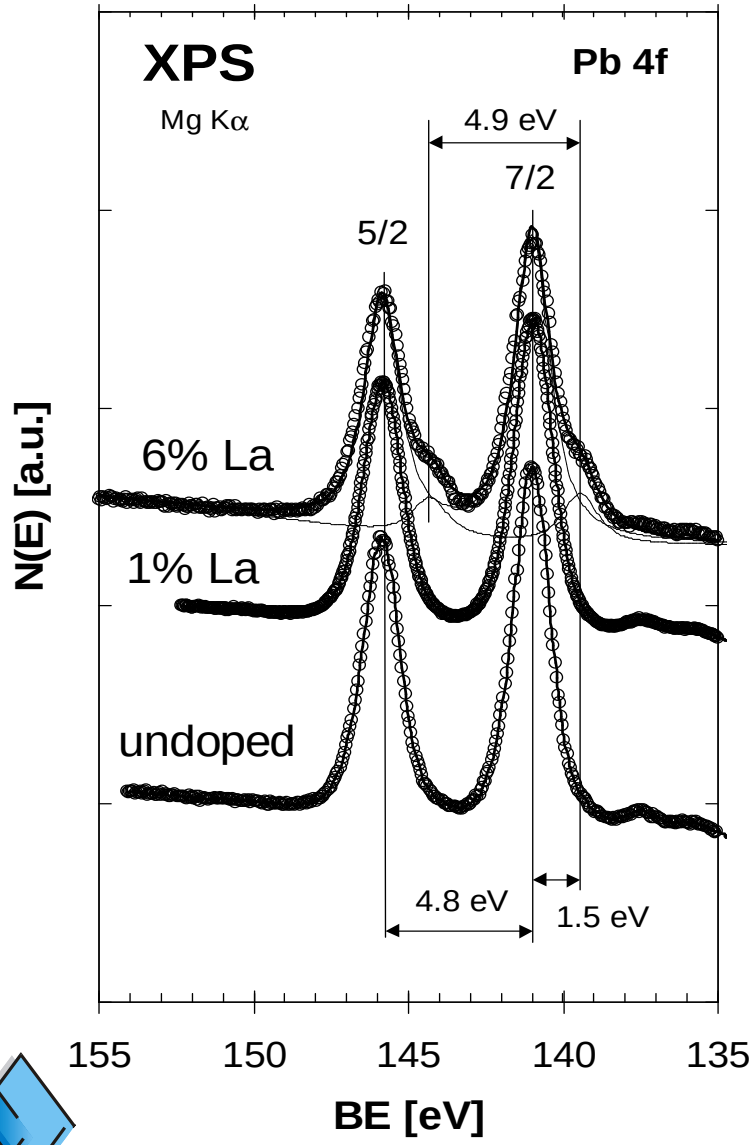
XPS
Pb 4f
Mg Kα
4.9 eV
7/2
5/2
6% La
1% La
undoped
4.8 eV
1.5 eV
N(E) [a.u.]
155
150
145
140
135
BE [eV]

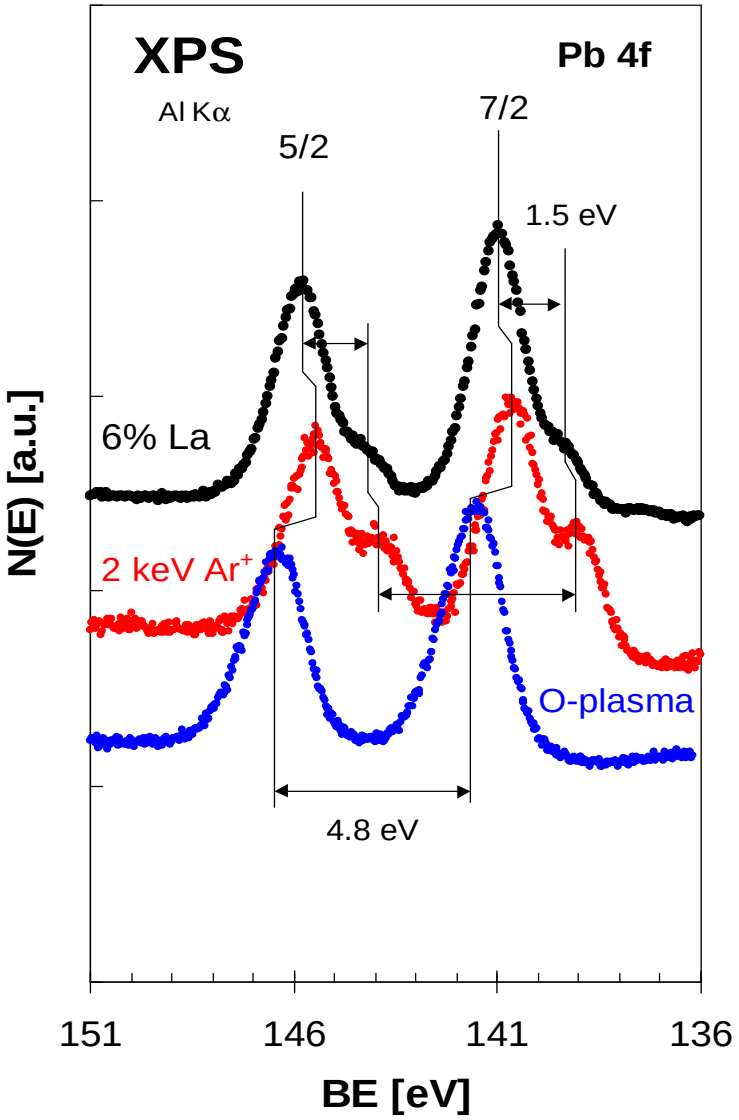
XPS
Pb 4f
Al Kα
7/2
5/2
1.5 eV
6% La
2 keV Ar+
O-plasma
4.8 eV
N(E) [a.u.]
151
146
141
136
BE [eV]

About the defect structure of PZT - compensation mechanisms

(i) Vacancy formation (e.g. for La^{3+}-, Nb^{5+}-doping):

La^{3+} on the A-site:

$$3\,Pb(Zr/Ti)O_3 + La_2O_3 \rightarrow 3(La^{\bullet}_{Pb})_{2/3}(V''_{Pb})_{1/3}(Zr/Ti)O_3 + 3\,PbO$$

$$3\,Pb(Zr/Ti)O_3 + 2\,La_2O_3 \rightarrow 4\,La^{\bullet}_{Pb}(V''''_{(Zr/Ti)})_{1/4}(Zr/Ti)_{3/4}O_3 + 3\,PbO$$

La^{3+} on the B-site:

$$2\,Pb(Zr/Ti)O_3 + La_2O_3 \rightarrow 2\,Pb\,La'_{(Zr/Ti)}(V^{\bullet\bullet}_O)_{1/2}O_{5/2} + 2(Zr/Ti)O_2$$

Nb^{5+} on the B-site:

$$Pb(Zr/Ti)O_3 + Nb_2O_5 \rightarrow 2\,Pb_{1/2}(V''_{Pb})_{1/2}Nb^{\bullet}_{(Zr/Ti)}O_3 + (Zr/Ti)O_2$$

$$5\,Pb(Zr/Ti)O_3 + 2\,Nb_2O_5 \rightarrow 5\,Pb(Nb^{\bullet}_{(Zr/Ti)})_{4/5}(V''''_{(Zr/Ti)})_{1/5}O_3 + 5(Zr/Ti)O_2$$

Nb^{5+} on the A-site:

$$5\,Pb(Zr/Ti)O_3 + Nb_2O_5 \rightarrow 5(Nb^{\bullet\bullet\bullet}_{Pb})_{2/5}(V''_{Pb})_{3/5}(Zr/Ti)O_3 + 5\,PbO$$

$$Pb(Zr/Ti)O_3 + 2\,Nb_2O_5 \rightarrow 4\,Nb^{\bullet\bullet\bullet}_{Pb}(V''''_{(Zr/Ti)})_{3/4}(Zr/Ti)_{1/4}O_3 + PbO$$

„electrical“ compensation mechanisms

(ii) Conduction states

allow a fraction of free e^- or h^+ in the material
multiple charge states of the defects
e.g. formation of Ti^{3+} polaron states

→think of the FE oxide as a wide band gap SC

Position of **E_F** determines defect charge states and defect formation enthalpies

The V_{Pb} related lifetime τ_2

first principle total energy calculations predict [1] several stable charge states of V_{Pb}

The existance of V_{Pb}-V_O bound complexes is unlikely (endothermic, negative binding energies), **However:**

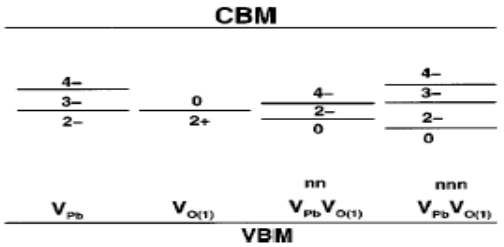

FIG. 1. Calculated ionization levels in the band gap for V_{Pb}, $V_{O(1)}$, and their complexes in $PbTiO_3$. Since the ionization levels for Pb-vacancy–O-vacancy complexes are nearly the same as the corresponding isolated vacancy levels, the formation of complexes is not stabilized by electron trapping. In the figure (nn) represents nearest-neighbor and (nnn) next-nearest-neighbor pairs, VBM stands for valence band maximum, and CBM for conduction band minimum.

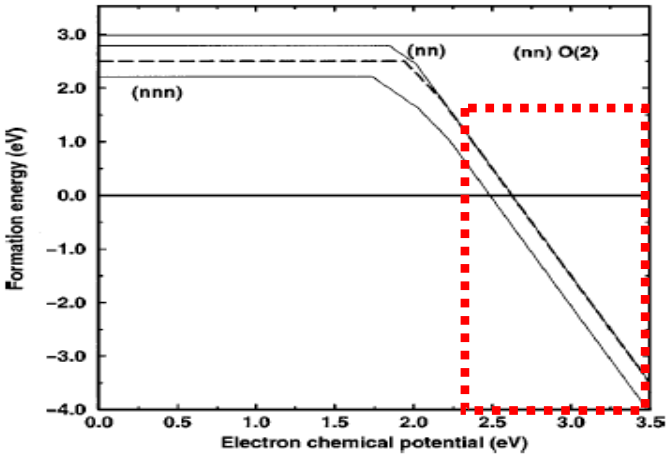

FIG. 2. Calculated formation energies as a function of Fermi energy for Pb-vacancy–O-vacancy pairs in $PbTiO_3$. The dashed line represents an isolated pair. Results for (nn) nearest-neighbor pair, (nnn) next nearest-neighbor V_{Pb}–$V_{O(1)}$ pair, and (nn) O(2) for a nearest-neighbor V_{Pb}–$V_{O(2)}$ pair are shown. Kinks in the lines are due to changes in the most stable charge states of pairs (ionization levels from Fig. 1). For the nearest-neighbor V_{Pb}–$V_{O(2)}$ pair, only the neutral charge state has been calculated (and is shown in the figure).

[1] S. Pöykö and D.J. Chadi APL **76** (2000) 499

Vacuum annealing

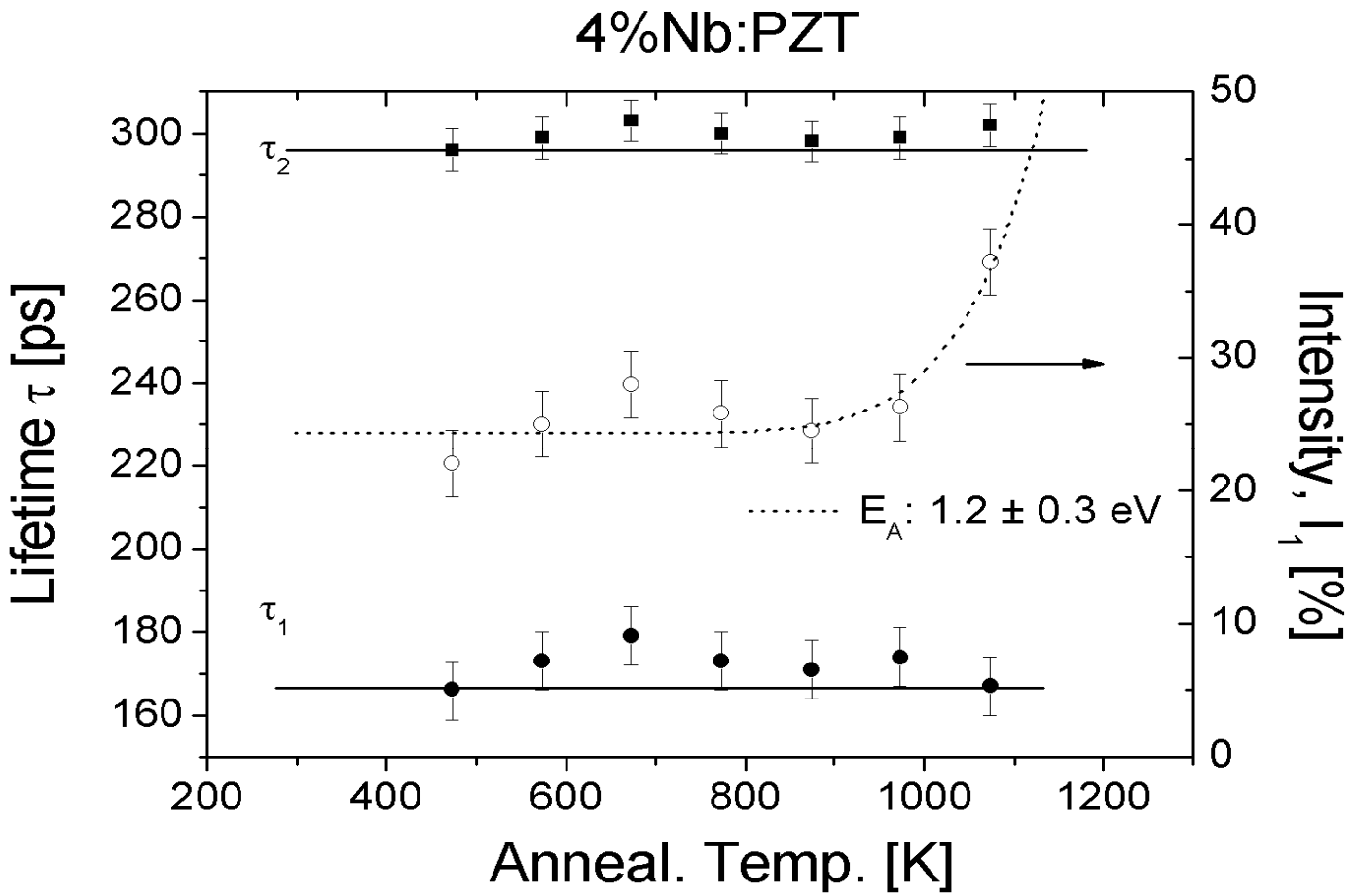

V_O trapping coefficient

(1) extremely high conc.

$k = \mu C$

e.g.: μ für Si: $\mu(V_{si}^{+})$: $6 \times 10^{13}\ s^{-1}$

$\mu(V_{si}^{0})$: $6 \times 10^{14}\ s^{-1}$

$\mu(V_{si}^{-})$: $5 \times 10^{15}\ s^{-1}$

(2) The charge is not 2+ !

Ti as a transition metal has empty 3d states

charge compensation

Temperature dependent trapping coefficient of positrons for different charge states

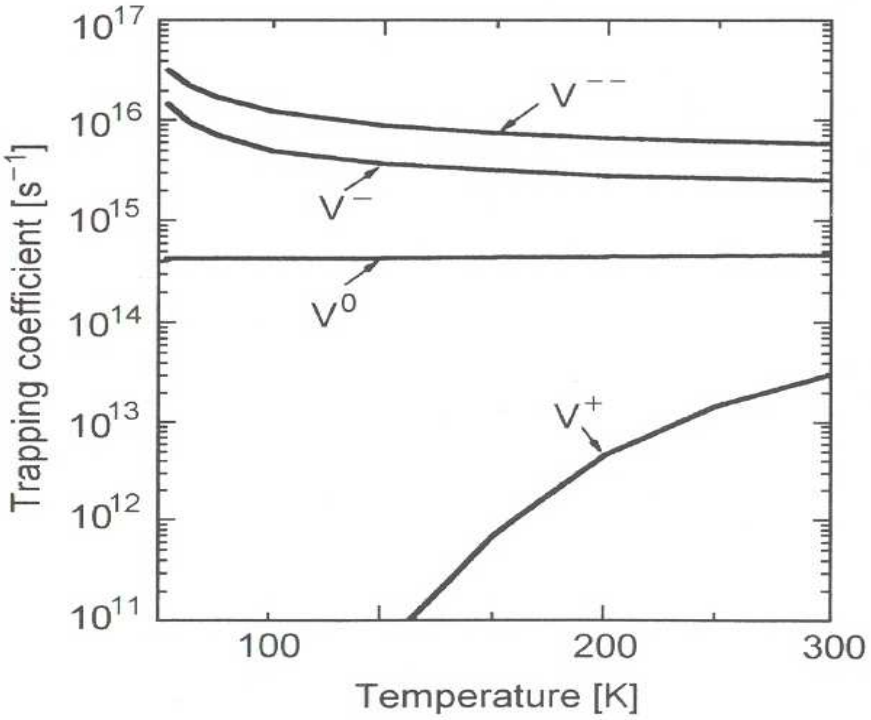

Calculation for semiconductors

Temperature dependant positron lifetimes

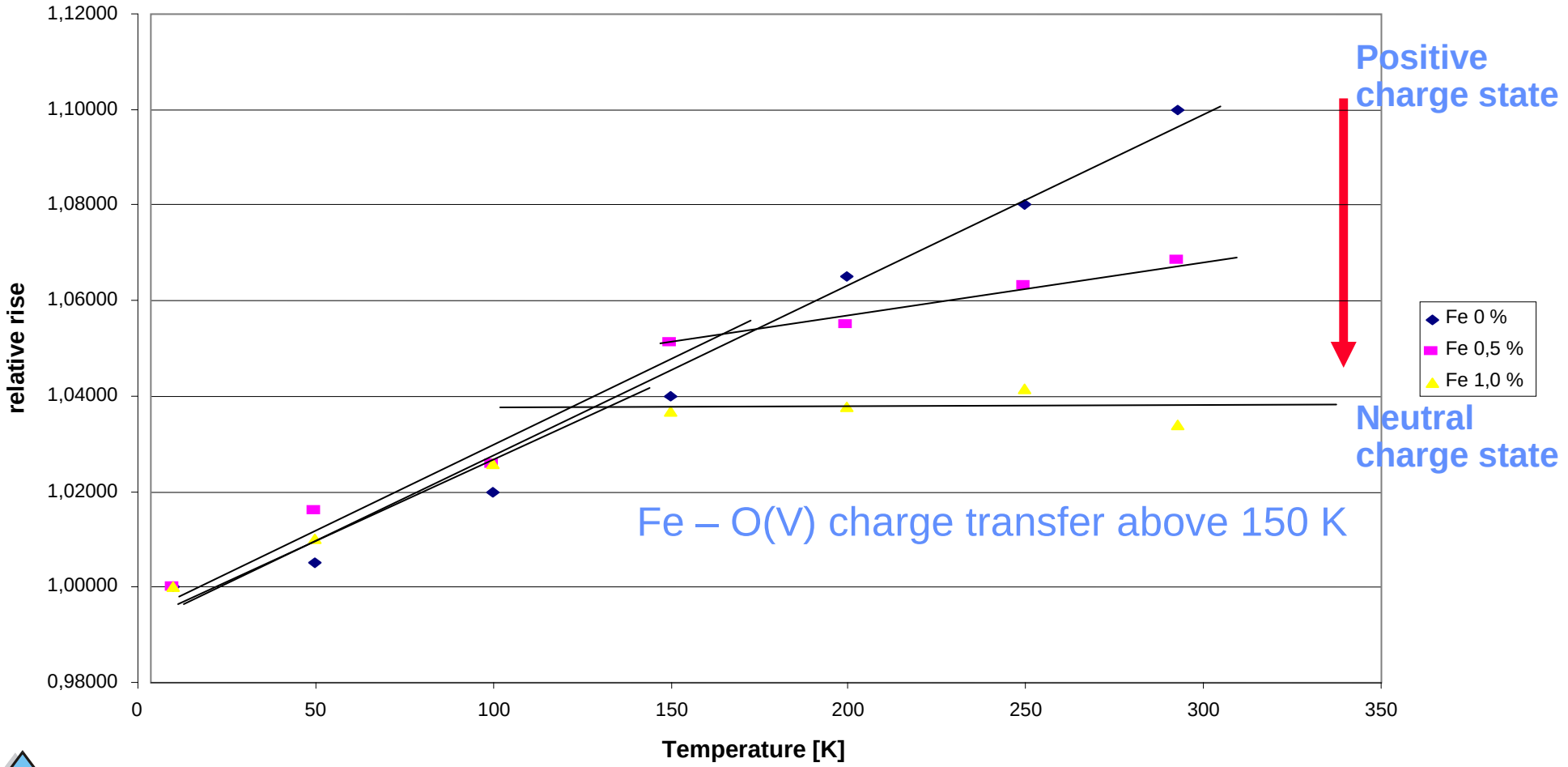

Mössbauer spectra of ^{57}Fe (0.5%):$Pb_1(Zr_{54}Ti_{46})_1O_3$ at different temperatures

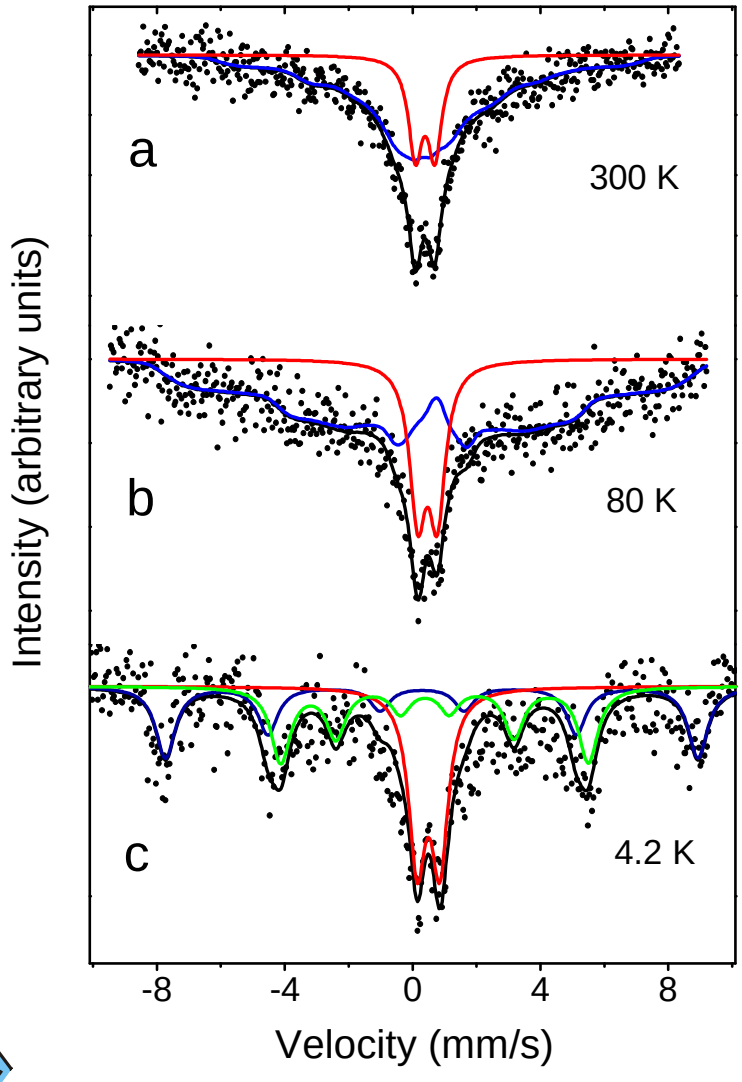

Doublet: Fe – O_v dipoles
Isomery shift: charge state Fe^{3+}
(in agreement with ESR)

Sextet: low spin relaxation
No magnetic intereaction because the large avarage distance between Fe atoms: distribution is homogenous

Interpreting the donor doping effects

– τ_2 is clearly associated to V_{Pb}

– τ_2 gradually increases from 255 to 305 ps with the dopant concentration

–for high donor concentrations the position of $E_F\uparrow$, which energetically favours associated V_O-V_{Pb} vacancy complexes

–defect concentrations are generally so high that saturation occurs

–τ_1 is stable at ~170 ps which corresponds to single V_O

–further evidence that τ_1 is not the bulk lifetime but associated with V_O comes from vacuum annealing experiments (defect formation enthalpy is about E~ 1eV)

–the charge state of V_O is probably not 2+

Microstructural Effects

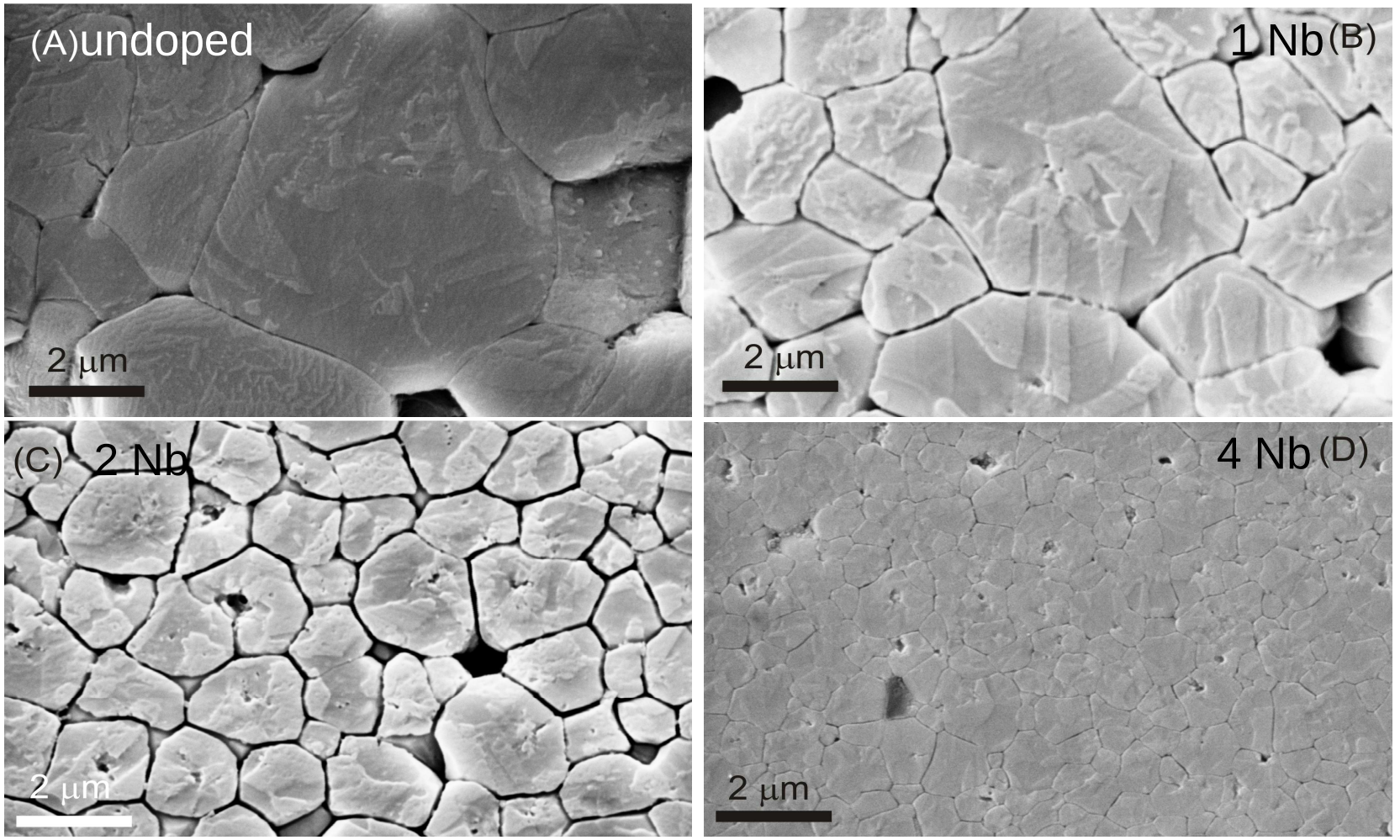

SEM images provided by H. Kungl

Oxygen Tracer Diffusion

Thermal indiffusion

^{18}O

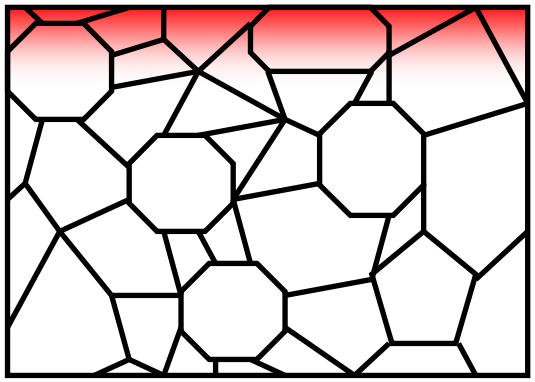

^{18}O Ion Implantation

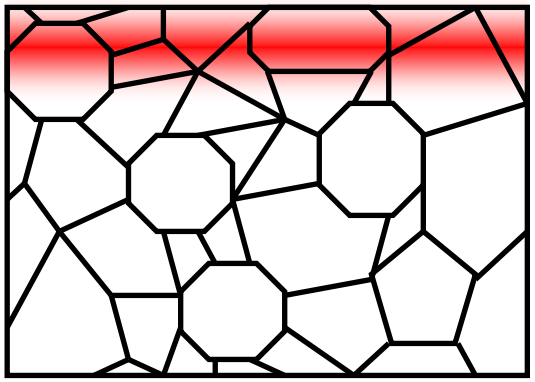

Annealing of the samples / Electrical fatigueing
depth profiling of the ^{18}O Tracer by means
of **SIMS** or **NRA** $^{18}O(p,\gamma)^{19}N$ E_{res} :151.2 ± 0.05 keV

^{18}O

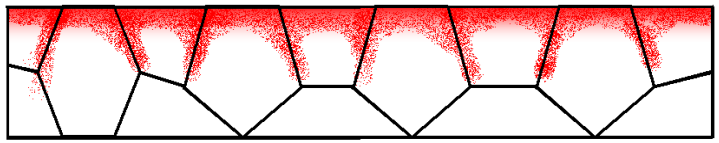

However using poly samples
GB contributions are apparent!

^{18}O-tracer Diffusion Experiments

Thermal indiffusion of ^{18}O is possible
However, limited temperature range (200-400ºC)
Alternative: ^{18}O ion implantation

Depth profiles include several fast diffusive components
D ranges from 7 x 10^{-19} - 2 x 10^{-15} cm^2/sec

Seperation of the components
Electric cycling mediated diffusion is in progress

^{18}Oxygen Tracer Diffusion

thermal ^{18}O exchange indiffusion 400ºC for 3 hrs. 2psi

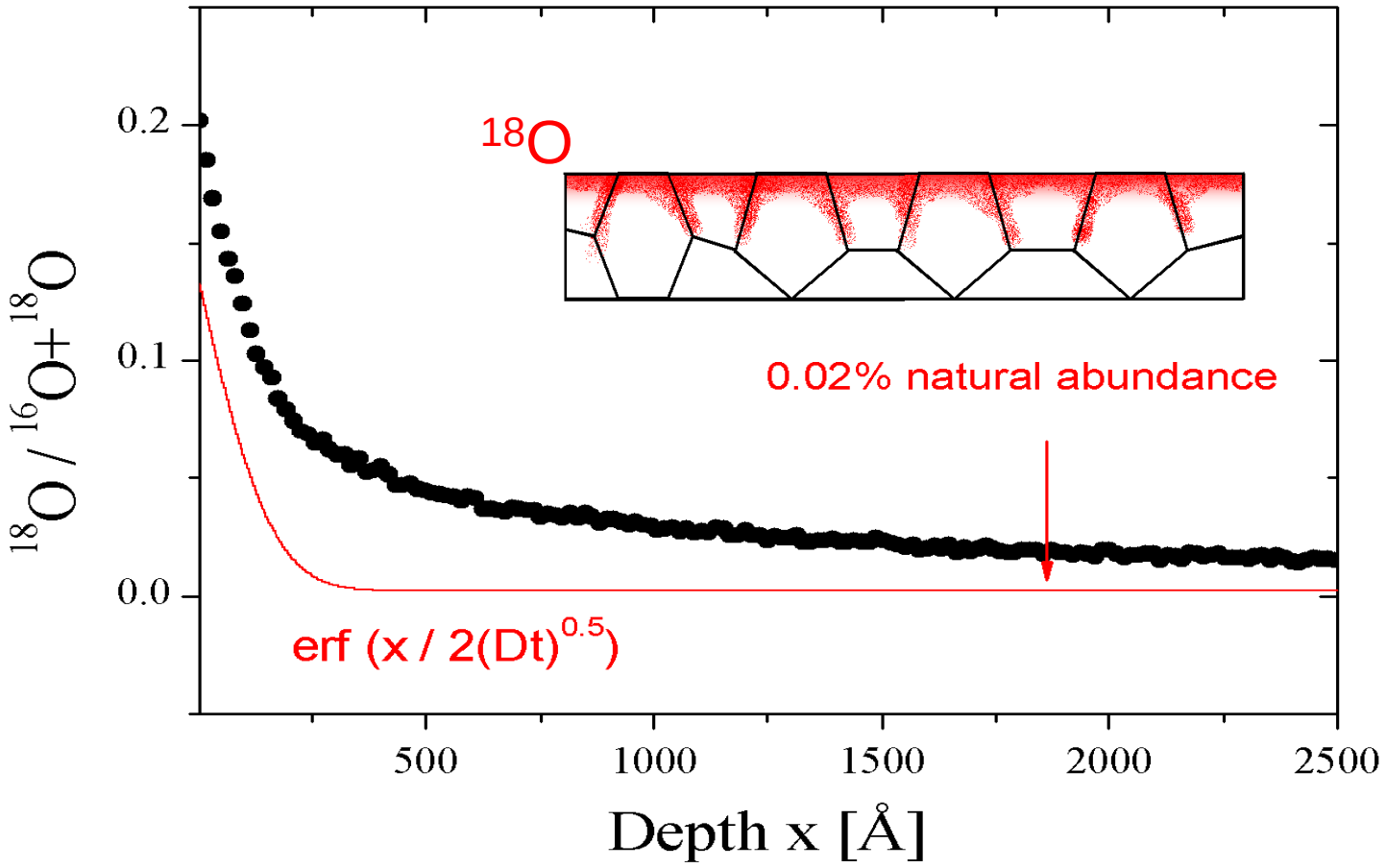

Principle of SIMS measurement

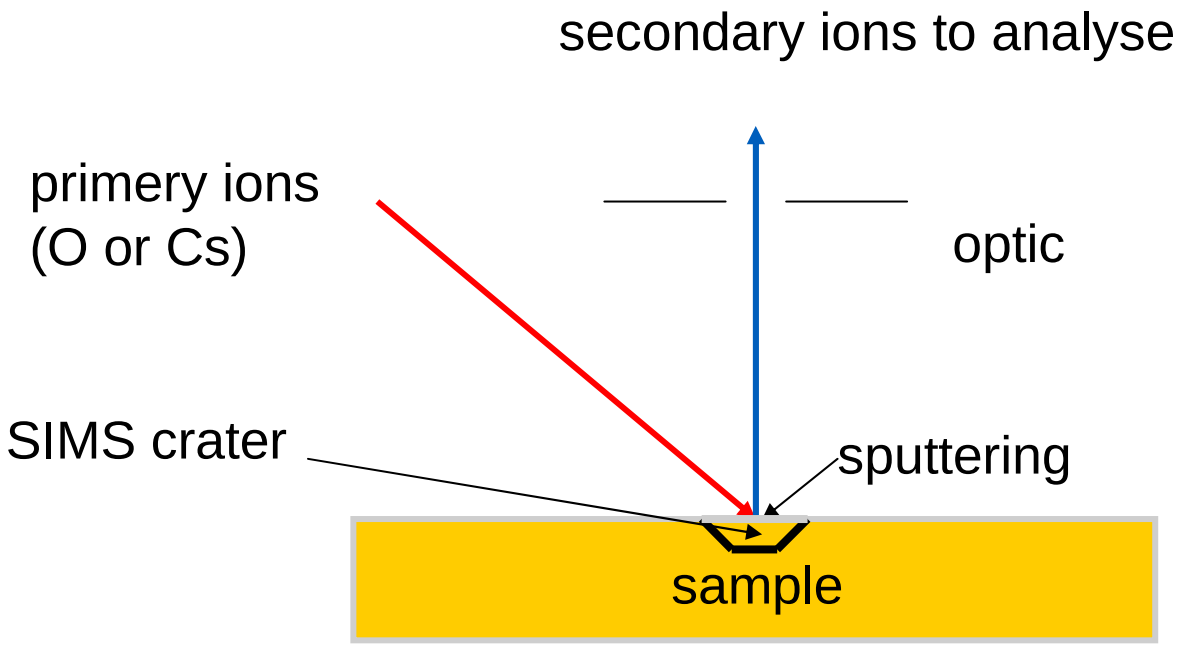

SIMS ^{18}O depth profiles in PZT (Pb-Zr-Ti-O) ferroelectric samples

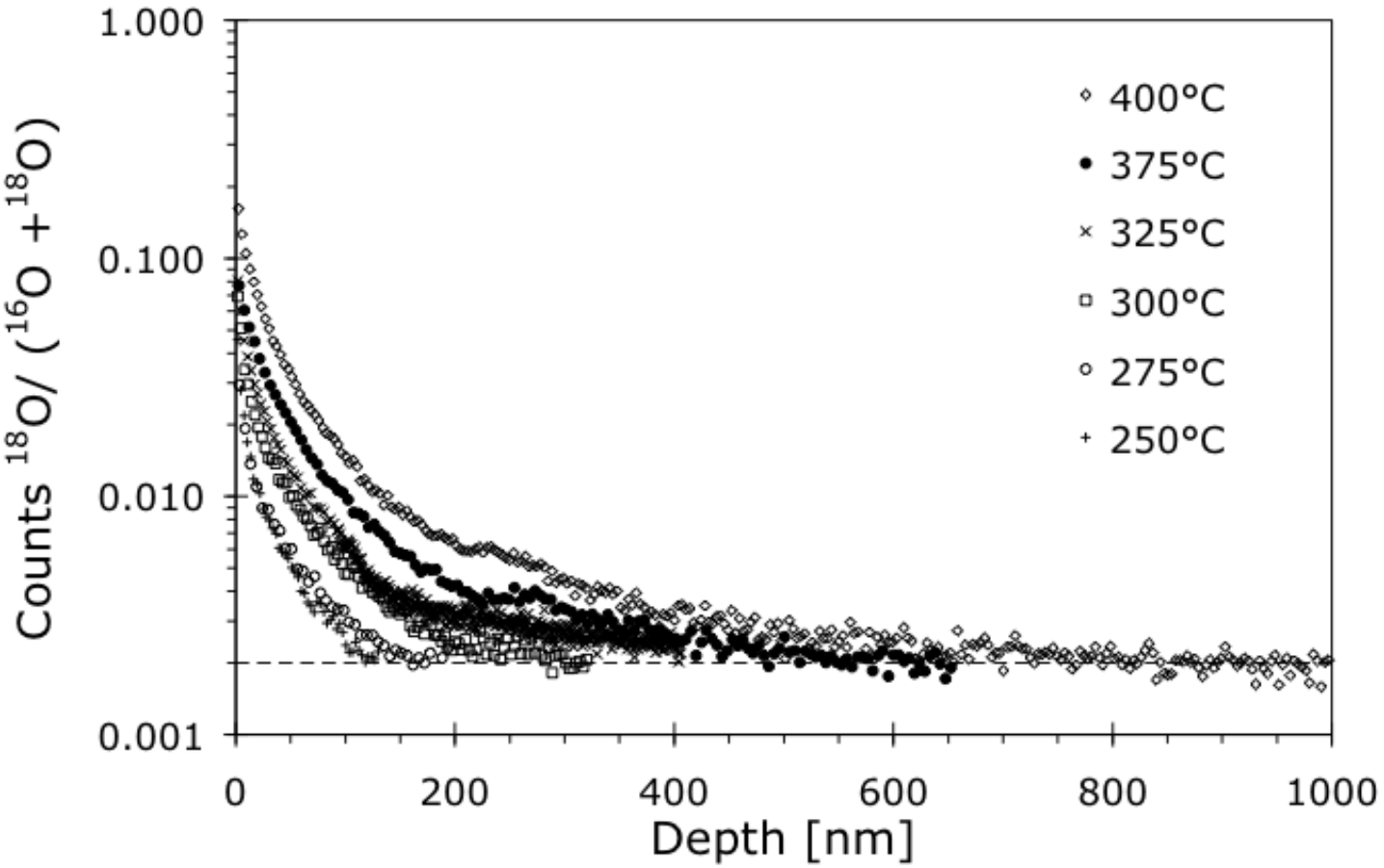

Activation enthalpies and chemical surface reaction for O in PZT

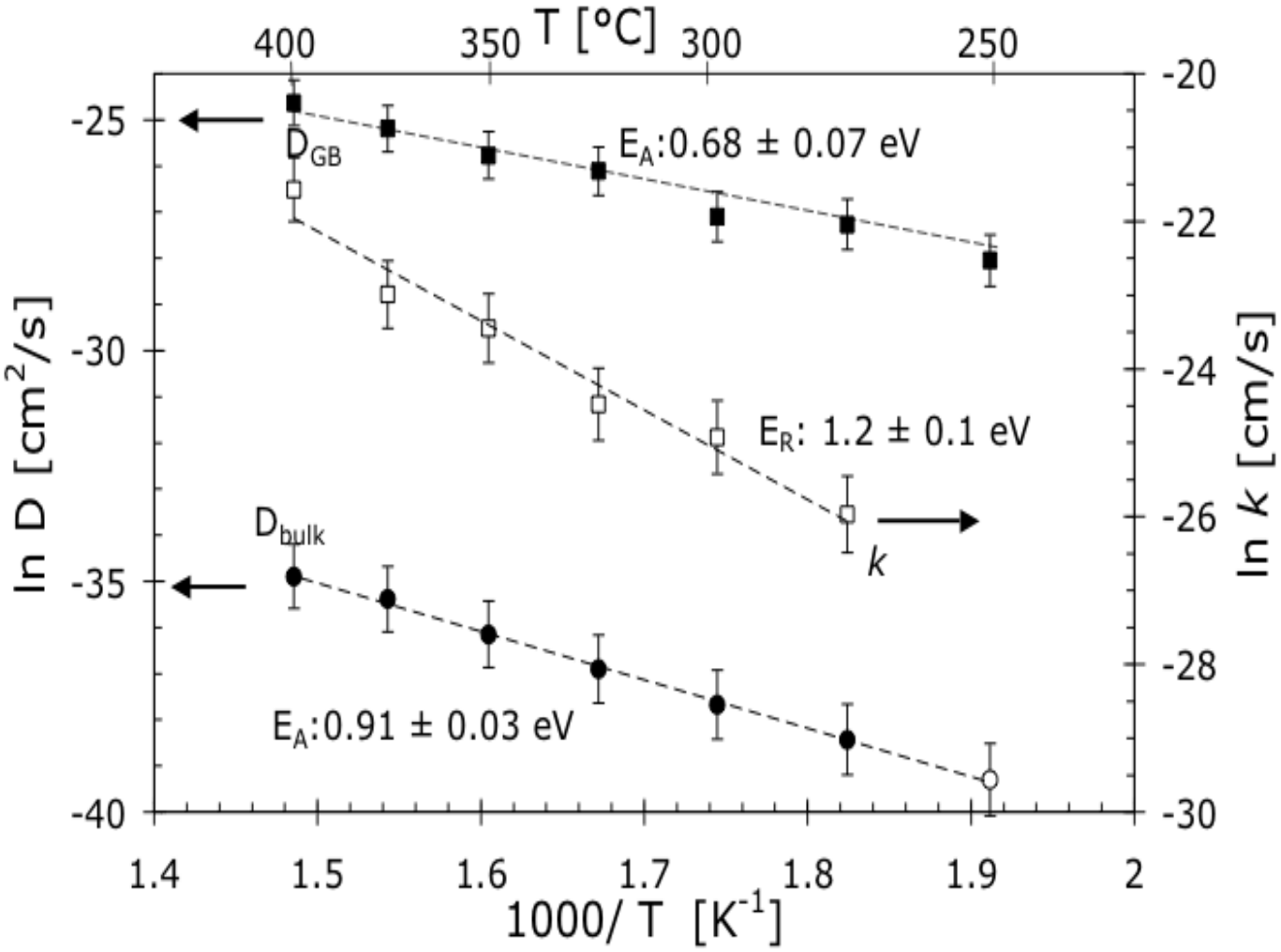

Oxygen Implantation

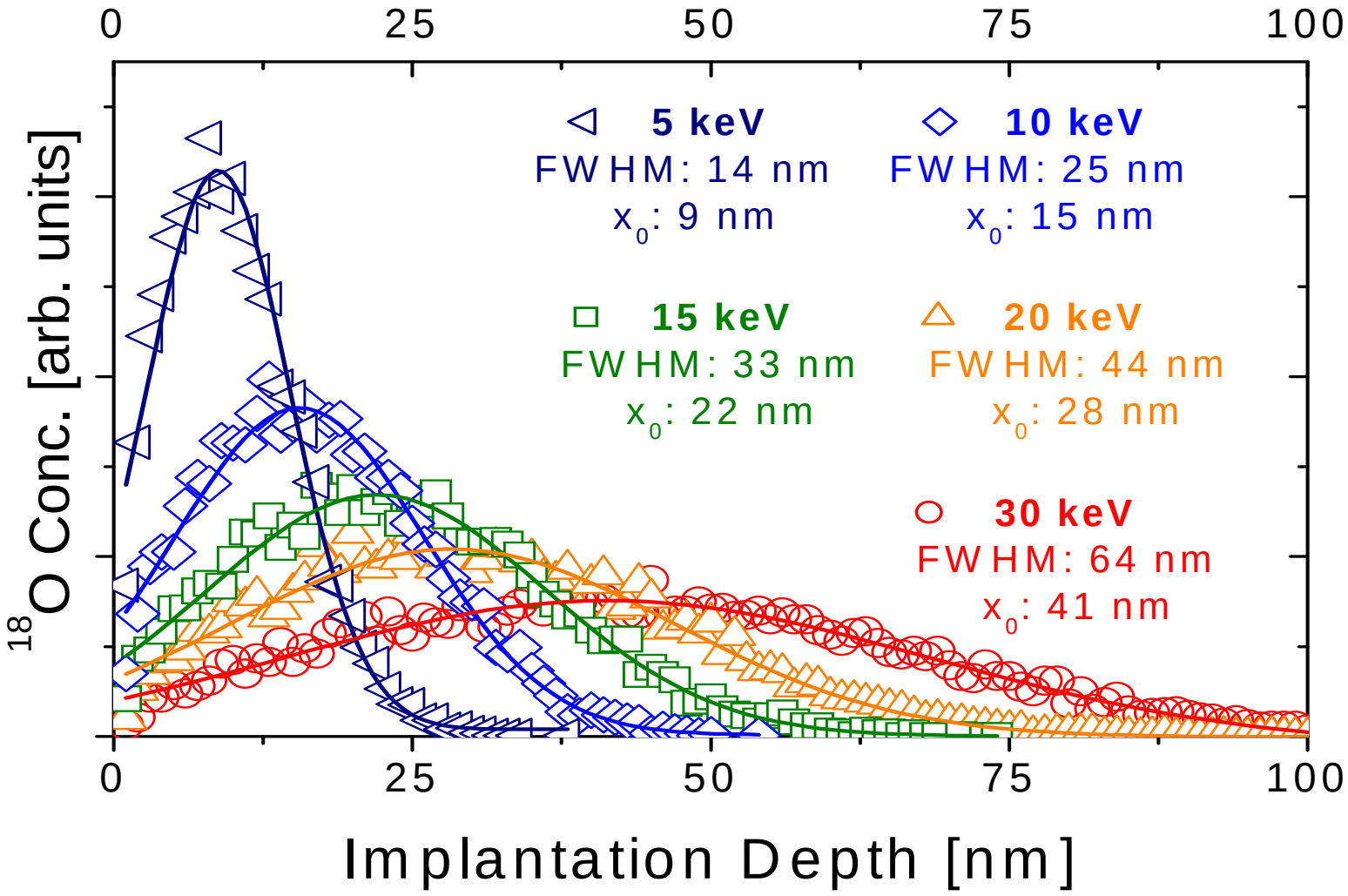

Summary and Conclusions

- **PAS** clearly shows that La as well as Nb doping yields to the saturation of lifetime component τ_2, supposedly belonging to $\tau(V_{Pb})$ ~300ps
- both dopants produce single Pb vacancies
- we suggest the existance of associated $V_{Pb}V_O$ vacancies in undoped samples, However $\tau(V_{Pb}V_O)^0 < \tau(V_{Pb})^{2-}$
- as τ_2 saturates, τ_{bulk} disappears, and I_2 drops, τ_1 can be attributed to $\tau(V_O)$ ~155 ps
- consequently the dopant also creates V_O
- Surprisingly V_O^{2+} are easily detectable with **PAS**